Journal of Organometallic Chemistry 694 (2009) 2705–2711

Contents lists available at ScienceDirect

Journal of Organometallic Chemistry

journal homepage: www.elsevier.com/locate/jorganchem

Novel iridium complex with carboxyl pyridyl ligand for dye-sensitized solar cells: High fluorescence intensity, high electron injection efficiency?

Zhijun Ning [a], Qiong Zhang [a,b], Wenjun Wu [a], He Tian [a,*]

[a] Key Laboratory for Advanced Materials and Institute of Fine Chemicals, East China University of Science and Technology, Meilong Road 130, Shanghai 200237, China
[b] Theoretical Chemistry, School of Biotechnology, Royal Institute of Technology, S-10691 Stockholm, Sweden

ARTICLE INFO

Article history:
Received 16 January 2009
Received in revised form 17 February 2009
Accepted 17 February 2009
Available online 28 February 2009

Keywords:
Dye sensitized solar cells
Photovoltaic material
Iridium complex
Luminescence

ABSTRACT

Novel iridium-based sensitizers Iridium(III) bis[2-phenylpyridinato-$N,C^{2'}$]-5-carboxylpicolinate) (**Ir1**), Iridium(III) bis[2-(naphthalen-1-yl) pyridinato-$N,C^{2'}$]-5-carboxyl-picolinate) (**Ir2**), Iridium(III) bis[2-phenylpyridinato-$N,C^{2'}$]-4,4′-(dicarboxylicacid)-2,2′-bipyridine (**Ir3**) were synthesized for sensitization of mesoscopic titanium dioxide injection solar cells. By changing the ligand, the absorption spectra can be extended and molar extinction coefficient was enhanced. The dye-sensitized nanocrystalline TiO_2 solar cells (DSSCs) based on dye **Ir3** showed the best photovoltaic performance: a maximum monochromatic incident photon-to-current conversion efficiency (IPCE) of 85%, a short-circuit photocurrent density (J_{sc}) of 9.59 mA cm^{-2}, an open-circuit photovoltage (V_{oc}) of 0.552 V, and a fill factor (*ff*) of 0.54, corresponding to an overall conversion efficiency of 2.86% under AM 1.5 sun light. Moreover, the HOMO and LUMO energy levels tuning can be conveniently accomplished by alternating the ligand. The high oxidative potential of **Ir3** enables it to be used along with Br^-/Br_3^- redox electrolyte and the photovoltage was found to be enhanced greatly.

1. Introduction

Dye-sensitized solar cells (DSSCs) have attracted intensive interest for their high performance in converting solar energy-to-electricity at low cost [1,2]. In DSSCs, dye molecules anchored to the surface of nanocrystalline TiO_2 absorb visible light and then inject electron into the conduction band of the TiO_2 in their excited states. Recently, the synthesis of transition-metal dye molecules for use as DSSCs sensitizers has received much attention. The photo-sensitizers based on Ru-complexes such as the black dye show record solar energy-to-electricity conversion efficiency of 11% [3–6]. Other metal complexes based dyes have also been used, including complexes of Pt [7–13], Fe [14], Os [15], Cu [16], and Re [17]. Recently, the utility of iridium (Ir) complex with PF_6^- counter ions as dye sensitizer in DSSCs was reported [18], yet, yielding low efficiency.

The photophysical and photochemical properties of Ir(III) complexes have been widely investigated in the last 2 decades [19,20]. These investigations are aimed to understand the energy and electron transfer processes in the excited state and to apply these principles to practical applications such as in solar energy conversion [18,21], organic light-emitting diode (OLED) [22–32], and sensors [33,34]. Ir(III) complexes are known to exhibit close to unity phosphorescence efficiency, which leads to the highest electroluminescence efficiency in OLED [35–48]. However, the application of Ir(III) complexes in DSSCs yielded extraordinarily low efficiency, although the quantum yield for conversion of absorbed photons to current in DSSCs based on Ir sensitizer is comparable to the ruthenium dyes [18]. Additionally, in solar cells based on the Ru dyes, the current production is based solely on injection from metal to-ligand charge transfer (MLCT). By contrast, it is possible to incorporate injection both from MLCT and ligand-to-ligand charge transfer (LLCT) for Ir(III) dyes [18]. The critical factors that limit the efficiency of Ir(III) dyes are low molar extinction coefficient and narrow absorption spectra. In this paper, we try to improve the conversion efficiency of Ir(III) dye by tuning the spectral overlap between the absorption spectra of Ir(III) dye and the solar spectrum and enhancing its molar extinction coefficient simultaneously.

2. Experimental

2.1. Chemicals and instruments

^{1}H NMR measurements were performed on a Brücker AM 500 spectrometer. Mass spectra were done with a HP5989 mass spectrometer. UV–Vis spectra were recorded on a Varian Cary 500 spectrophotometer and fluorescence emission spectra were on a Varian Cary Eclipse fluorescence spectrophotometer. Cyclic voltammetry was performed using a Potentiostat/Galvanostat Model K0264 (Princeton Applied Research). Anhydrous CH_2Cl_2 was used as the

* Corresponding author. Tel./fax: +86 21 64252288.
E-mail address: tianhe@ecust.edu.cn (H. Tian).

0022-328X/$ - see front matter © 2009 Elsevier B.V. All rights reserved.
doi:10.1016/j.jorganchem.2009.02.016

solvent under inert atmosphere, and 0.1 M TBAHFP (tetra(*n*-butyl)ammonium hexafluorophosphate) was used as the supporting electrolyte. A platinum disk electrode was used as the working electrode, a platinum wire the counter electrode, and a saturated Ag/AgCl reference electrode.

2.2. Preparation of dye-sensitized nanocrystalline TiO_2 electrodes

The preparation of dye-sensitized TiO_2 electrode was prepared according to the procedure reported in the literature. TiO_2 colloidal dispersion was made according to the Ref. [49] employing commercial TiO_2 (P25, Degussa AG, Germany). Films of nanocrystalline TiO_2 colloidal on FTO were prepared by sliding a glass rod over the conductive side of the FTO. Sintering was carried out at 450 °C for 30 min. Before immersion in the dye solution, these films were soaked in the 0.2 M aqueous $TiCl_4$ solution overnight in a closed chamber, which has been proved to increase the short-circuit photocurrent significantly [49]. The thickness of the TiO_2 film was about 12.5 μm. After being washed with deionized water and fully rinsed with ethanol, the films were heated again at 450 °C followed by cooling to 80 °C and dipping into a 3×10^{-4} M solution of dyes in ethanol for 12 h at room temperature. The dye-coated TiO_2 film, as working electrode, was placed on top of an FTO glass as a counter electrode, on which Pt was sputtered. The redox electrolyte was introduced into the inter-electrode space by capillary force.

2.3. Photoelectrochemical measurements

The photoelectrochemical experiments were performed in sandwich-type two-electrode cells. The dye-coated film was used as working electrode, platinic FTO glass as counter electrodes and 0.4 M 1-methyl-3-propyl imidiazolium iodide, 0.3 M LiI, and 0.03 M I_2 in mixed solution of acetonitrile and 3-methyl-2-oxazolidinone (volume ratio: 9:1) as electrolyte. The photocurrent action spectra were measured with a Model SR830 DSP Lock-In Amplifier and a Model SR540 Optical Chopper (Stanford Research Corporation, USA), a 7IL/PX150 xenon lamp and power supply, and a 7ISW301 Spectrometer. The irradiation source for the photocurrent density–voltage (*J*–*V*) measurement is an AM 1.5 solar simulator (Newport-91160-1000). The incident light intensity was 100 mW cm^{-2} calibrated with a standard silicon solar cell. The tested solar cells were masked to a working area of 0.15 cm^2. Volt–current characteristic were performed on Model 2400 Sourcemeter (Keithley Instruments, Inc. USA).

2.4. Synthesis

2.4.1. General procedure for the synthesis of **Ir1**, **Ir2**, and **Ir3**

Chloro-bridged dimer complex [50] (0.1 mmol) and pyridine-2,5-dicarboxylic acid (0.11 mmol) were added in a mixture of Na_2CO_3 (88.8 mg, 0.83 mmol), and 2-ethoxyethanol (10 mL). After refluxed for 24 h under argon atmosphere, the solution was cooled to room temperature and poured into water. The precipitate was filtered off and washed with water, hexane, and ether. The crude products were applied to column chromatography on silica gel, eluting with methylene chloride and ethanol to provide the desired product.

2.4.2. Iridium(III) bis[2-phenylpyridinato-N,$C^{2'}$]-5-carboxylpicolinate (**Ir1**)

^{1}H NMR (500 MHz, DMSO-d_6): δ 6.51 (d, 1H, *J* = 6.4 Hz), 6.71 (d, 1H, *J* = 6.4 Hz), 7.08–7.33 (m, 5H), 7.52 (m, 1H), 7.71 (s, 1H), 7.83 (m, 1H), 7.97 (m, 2H), 8.10 (s, 2H), 8.25 (m, 2H), 8.67 (m, 1H), 8.82 (m, 1H), 8.98 (m, 1H). ^{13}C NMR (125 MHz, DMSO-d_6): δ 119.2, 119.3, 120.7, 121.0, 122.7, 123.2, 124.1, 124.8, 126.6, 128.9, 129.6, 131.7, 131.9, 137.9, 138.0, 138.4, 139.8, 143.9, 144.6, 147.5, 148.1, 149.4, 150.2, 150.7, 165.5, 167.0, 167.8, 171.9. HRMS (*m*/*z*): $[M+H]^+$ calcd. for $C_{29}H_{21}N_3O_4Ir$, 666.1138. Found: 666.1124.

2.4.3. Iridium(III) bis[2-(naphthalen-1-yl)pyridinato-N,$C^{2'}$]-5-carboxylpicolinate (**Ir2**)

^{1}H NMR (500 MHz, DMSO-d_6): δ 6.51 (d, 1H, *J* = 6.4 Hz), 6.71 (d, 1H, *J* = 6.4 Hz), 7.08–7.33 (m, 5H), 7.52 (m, 1H), 7.71 (s, 1H), 7.83 (m, 1H), 7.97 (m, 2H), 8.10 (s, 2H), 8.25 (m, 2H), 8.67 (m, 1H), 8.82 (m, 1H), 8.98 (m, 1H). ^{13}C NMR (125 MHz, DMSO-d_6): δ 121.1, 121.5, 121.9, 122.5, 122.7, 122.8, 123.0, 123.2, 127.0, 127.2, 128.6, 129.4, 129.5, 129.7, 130.5, 130.6, 130.7, 130.8, 130.9, 131.3, 136.4, 137.4, 138.4, 148.2, 149.0, 151.0, 154.8, 156.1, 167.4, 168.0, 171.5. HRMS (*m*/*z*): $[M+H]^+$ calcd. for $C_{37}H_{25}N_3O_4Ir$, 766.1451. Found: 766.1485.

2.4.4. Iridium(III) bis[2-phenylpyridinato-N,$C^{2'}$]-4,4′-(dicarboxylicacid)-2,2′-bipyridine (**Ir3**)

^{1}H NMR (500 MHz, DMSO-d_6): δ 6.19 (d, 2H, *J* = 7.2 Hz), 6.89 (t, 2H, *J* = 7.2 Hz), 7.00 (t, 2H, *J* = 7.2 Hz), 7.14 (t, 2H, *J* = 7.0 Hz), 7.62 (d, 2H, *J* = 5.6 Hz), 7.80 (d, 2H, *J* = 5.2 Hz), 7.84 (d, 2H, *J* = 5.6 Hz), 7.93 (m, 4H), 8.25 (d, 2H, *J* = 8.4 Hz), 8.82 (S, 2H), ^{13}C NMR (125 MHz, DMSO-d_6): δ 121.0, 123.7, 124.5, 125.1, 126.0, 128.5, 131.5, 132.8, 139.6, 145.2, 150.0, 150.1, 151.6, 151.7, 157.7, 169.2, 169.9. HRMS (*m*/*z*): $[M]^+$ calcd. for $C_{34}H_{24}N_4O_4Ir$, 743.1404. Found: 743.1421.

3. Results and discussion

3.1. Synthesis, spectra and electrochemical properties

The synthetic route was shown in Scheme 1. It is found that the reaction of the chloro-bridged dimer complex with ligand pyridine-2,6-dicarboxylic acid did not yield the carboxyl substituted complex, which might be caused by the coordination between Ir(III) and the two neighboring carboxyl groups of pyridine-2,6-dicarboxylic acid. However, the reaction with ligand pyridine-2,5-dicarboxylic acid afforded the final complex with high yield.

Absorption spectra of all compounds in dilute solution of ethanol are shown in Fig. 1. Absorption data are summarized in Table 1. The absorption spectra of these compounds show intense bands ($\varepsilon > 10^4$ M^{-1} cm^{-1}) in the ultraviolet region between 200 and 300 nm. These bands are attributed to spin-allowed π–π^* ligand-centered (LC) transitions [51,52]. The less intense, lower energy absorption features from 300 to 600 nm are due to charge-transfer (CT) transitions. Two types of CT transitions can be distinguished in the spectra: bands of moderate intensity between 300 and 400 nm may be assigned to MLCT overlapping with LLCT transitions; and transitions with much weaker intensity in the visible region are tentatively assigned to ^{3}MLCT, mixed with significant $^3\pi\pi$ transition character [53].

The molar extinction coefficient of **Ir2** is considerably higher than **Ir1** and **Ir3**, implying that extended π-conjugation is favorable for the enhancement of the molar extinction coefficient. The maximum absorption wavelength within this series is in the order of **Ir2** > **Ir3** > **Ir1**, which shows that the absorption spectra can be extended by extending the conjugation ligand size. The absorption spectra of the sensitizers on TiO_2 film are shown in Fig. 2. There is no distinct shift of the absorption spectra after adsorbed on the TiO_2 film, indicative of no serious aggregation. Compound Ir3 has the highest absorbance in the long wavelength region for its relatively high dye loading and molar extinction coefficient in this region (Table 1).

All complexes were found to emit in air-equilibrated ethanol solutions at room temperature. The luminescence results are gath-

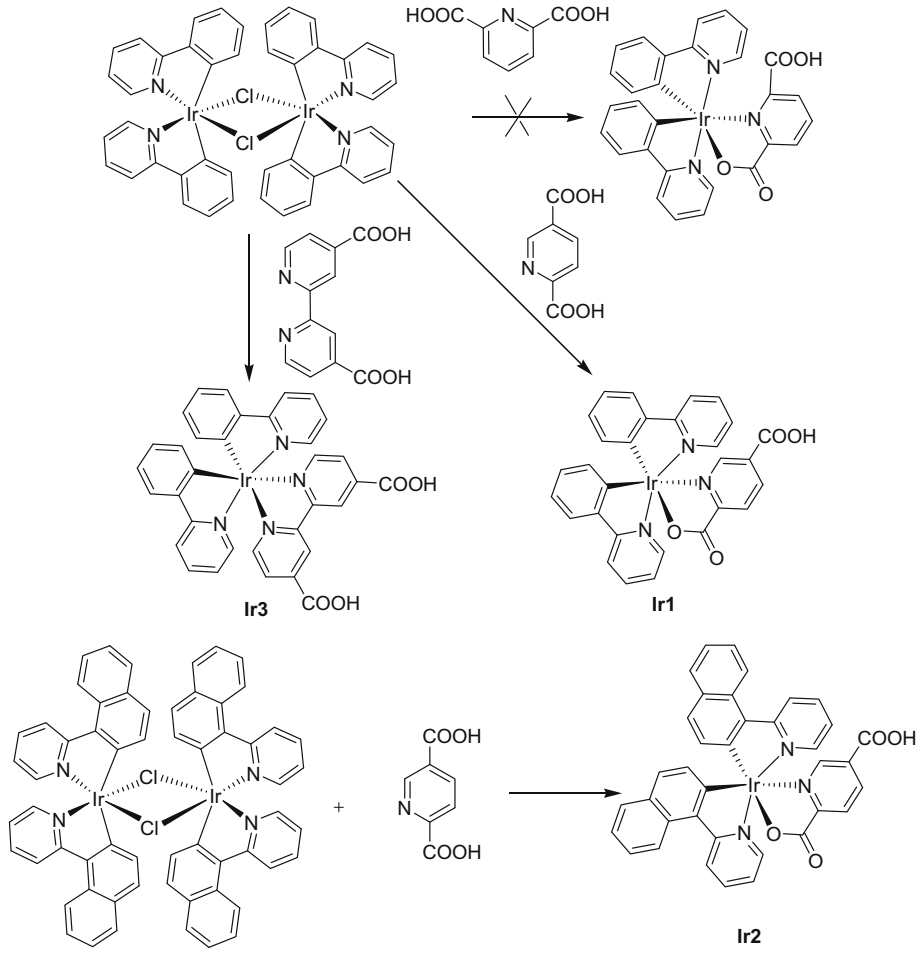

Scheme 1. Synthesis of the sensitizers.

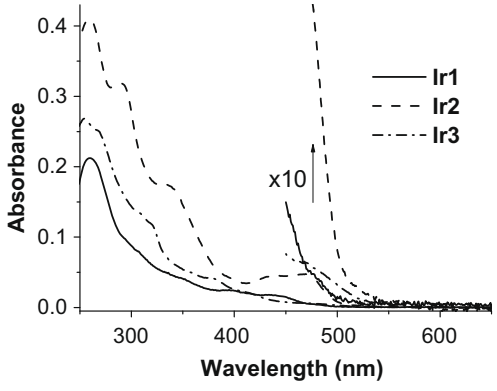

Fig. 1. Absorption spectra of dyes in ethanol (1×10^{-5} M).

ered in Table 1. The emission spectra are illustrated in Fig. 3. The quantum yield of **Ir1** and **Ir2** is dramatically lower than **Ir3**, which may be caused by the weaker metal–ligand bonding strength of the carboxyl pyridine group [53].

To evaluate the possibility of electron transfer from the excited dye molecule to the conductive band of TiO_2, cyclic voltammograms were performed in CH_2Cl_2 solution, using 0.1 M tetrabutylammonium hexafluorophosphate as the supporting electrolyte (Fig. 4). The photoelectrodes adsorbed with sensitizers were used to replace the working electrode. A summary of the redox potentials, measured relative to an internal ferrocene reference, is listed in Table 1. The oxidation potential values for **Ir1**, **Ir2**, and **Ir3** are 1.12, 1.02 and 1.48 V, respectively, all higher than I_3^-/I^-electrolyte (0.53 V), which can ensure effective dye regeneration process [54]. It is noteworthy that the oxidation potential of **Ir3** is even higher than the redox electrolyte Br_3^-/Br^- (1.09 V), which makes it possible to be used along with the Br^-/Br_3^- redox electrolyte [55]. Judging from the LUMO value, the excited state energy levels for the products are much higher than the bottom of the conduction band of TiO_2 (−4.4 eV), indicating that the electron injection process from the excited dye molecule to TiO_2 conduction band is energetically viable.

3.2. Quantum chemical calculation

To gain insight into the geometrical and electronic properties of these dyes, we mimicked the optimized geometries of **Ir1** and **Ir2** (Fig. 5) with GAUSSIAN 03 program [56], using hybrid density functional theory (B3LYP) and 6-31G* basis set for all atoms except Ir, for which Lanl2DZ-ECP was used. The optimized structure shows that all dihedral angles formed between two ligands are nearly perpendicular between each other, which is similar with the configuration of classic green emitter Alq_3 [57]. Such kind of starburst configuration can prohibit the aggregation effectively in solid state. The HOMO of these compounds is delocalized over the 2-phenyl-pyridine moiety. The LUMO is a π^* orbital delocalized

Table 1
Photophysical and electrochemical parameters of the dyes.

Complex	Absorption		Emission		HOMO (eV)	LUMO (eV)
	λ_{max} (nm)	ε (M^{-1} cm^{-1})	λ_{max} (nm)	Φ		
Ir1	260	21250	607	0.0024	−5.42	−2.94
	305	8103				
	397	2512				
	438	1824				
Ir2	258	40944	587	0.0067	−5.32	−3.00
	289	34954				
	335	17536				
	438	4405				
	471	4544				
Ir3	254	27100	582	0.38	−5.78	−3.43
	266	25528				
	317	12681				
	376	4405				
	413	2549				

across the 5-carboxylpicolinate group. The completely separated distribution of HOMO and LUMO orbitals indicates that photoexcitation may lead to an efficient intramolecular charge separation with an effective photocurrent generation [5].

To understand the excited states giving rise to the optically active absorption bands in the visible region, we performed TDDFT excited states calculations at the same level theory in vacuo with the B3LYP/6-31G*/Lanl2DZ-ECP optimized ground-state geometries. The lowest transitions of **Ir1** and **Ir2** are listed in Table 2. The first transitions (S_1) correspond to a charge-transfer excitation from the phenylpyridine HOMO to the LUMO, localized on carboxylpyridine acceptor. The S_1 oscillation strengths of **Ir1** and **Ir2** are low, and **Ir2** is larger than **Ir1**, which are all in accordance with the experiment value (Table 2).

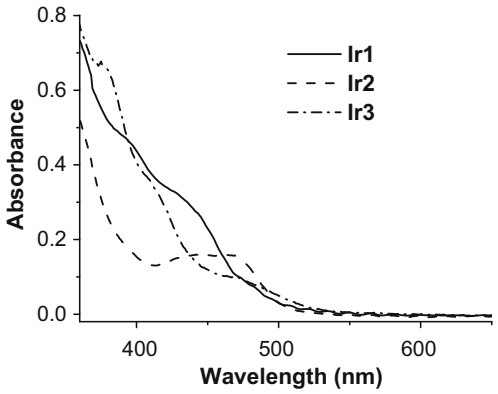

Fig. 2. Absorption spectra of dyes on TiO_2 film.

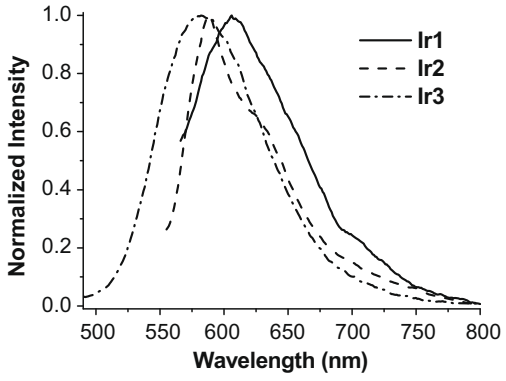

Fig. 3. Normalized emission spectra of dyes in ethanol (excited at 440 nm).

3.3. Cell performance

Fig. 6 shows the incident monochromatic photon-to-current conversion efficiency (IPCE) obtained with a sandwich cell using 0.4 M 1-methyl-3-propyl imidiazolium iodide, 0.3 M LiI, and 0.03 M I_2 in mixed solution of acetonitrile and 3-methyl-2-oxazolidinone (volume ratio: 9:1) as electrolyte. The IPCE data of **Ir3** sensitizer plotted as a function of excitation wavelength exhibit a strikingly high efficiency of 76% at 490 nm. The IPCE spectra of them are consistent with the absorption spectra on the TiO_2 film.

The light harvesting efficiency (LHE) can be related to the molar extinction coefficient by Eq. (I), where Γ is the surface coverage in mol/cm^2 and ε is the dye molar absorption coefficient in units of M^{-1} cm^{-1} at wavelength λ [49]

$$\mathrm{LHE}(\lambda) = 1 - 10^{-[1000(\mathrm{cm^3\ L^{-1}})\cdot\varepsilon(\mathrm{mol^{-1}\ L\ cm^{-1}})\cdot\Gamma(\mathrm{mol\ cm^{-2}})]} \quad \text{(I)}$$

The quantum yield for conversion of absorbed photons to current in DSSCs can be calculated by Eq. (II)

$$\phi(\lambda) = \mathrm{IPCE}(\lambda)/\mathrm{LHE}(\lambda) \quad \text{(II)}$$

The calculated quantum yields at 440 nm are 1.0, 0.49, and 0.43 for **Ir3**, **Ir2**, and **Ir1,** respectively. This order is consistent with their photoluminescence quantum yields listed in Table 1. The phosphorescence lifetime of **Ir3** was measured both in solution and on the TiO_2 film (Fig. 7). It was found that the lifetime dramatically decreased on the TiO_2 film, which means that the excited state elec-

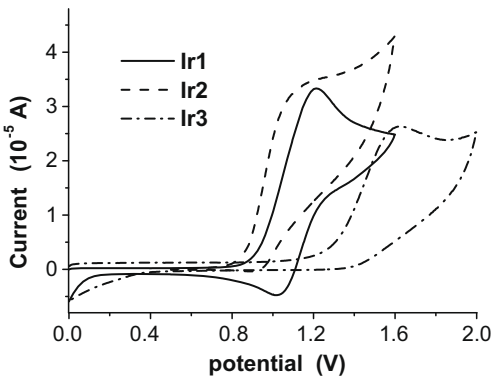

Fig. 4. Oxidative cyclic voltammogram of dyes adsorbed on the electrode coated with a thin layer of TiO_2.

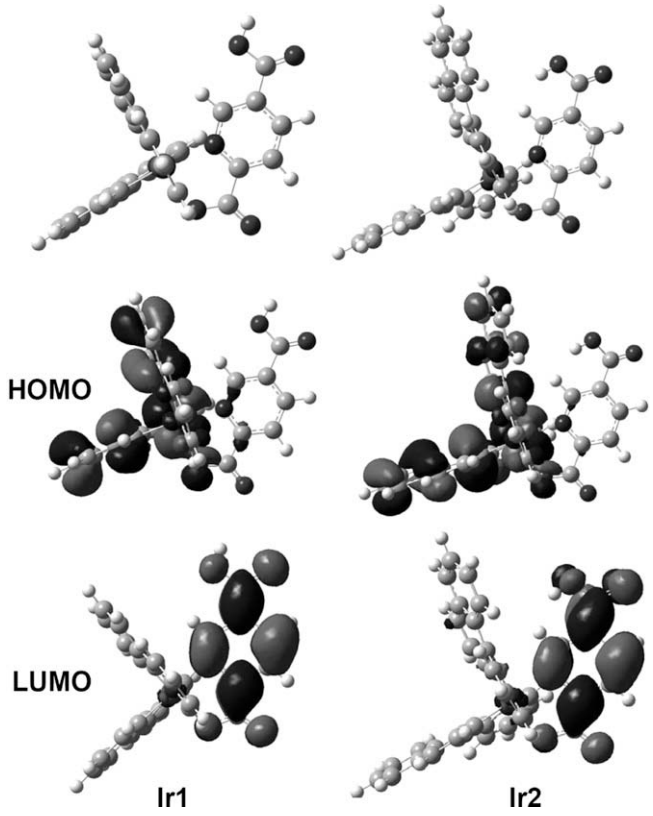

Fig. 5. Optimized ground-state geometries and isodensity surface plots of the HOMO and LUMO of **Ir1** and **Ir2**.

Table 2
Calculated TDDFT excitation energies for the lowest transitions (eV, nm), oscillator strengths (*f*), composition in terms of molecular orbital contributions.

Compounds	State	Composition[a]	*E* (eV, nm)	*f*
Ir1	S_1	99% H → L	2.30(540)	0.0007
	S_2	94% H → L−1	2.82(440)	0.0316
	S3	92% H+1 → L	2.87(432)	0.0072
Ir2	S_1	96% H → L	2.34(531)	0.0022
	S_2	91% H → L−1	2.63(472)	0.0397
	S_3	83% H → L−2	2.86(434)	0.0229
		5% H+1 → L		

[a] H = the highest occupied molecular orbital, L = the lowest unoccupied molecular orbital, H+1 = the next highest occupied molecular orbital, or HOMO+1, L−1 = the next lowest unoccupied molecular orbital, or LUMO−1. L−2 = LUMO−2.

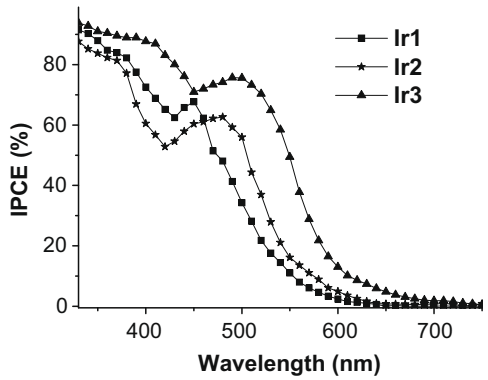

Fig. 6. Photocurrent action spectra of the TiO_2 electrodes sensitized by dyes.

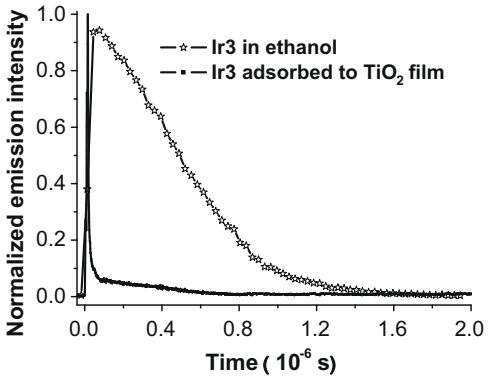

Fig. 7. Emission decays of the **Ir3** in ethanol and after adsorbed on TiO_2.

trons were injected into semiconductor effectively [58]. It was speculated that the radiation decay of the excited state electron was replaced by electron injection into TiO_2 semiconductor. The high luminescence efficiency indicates that there is less nonradiative deactivation process caused by the vibration or aggregation, which might also debase the electron injection efficiency in DSSCs [5,59]. Therefore, it can be concluded that the high luminescence efficiency of the sensitizer is favorable to achieve high electron injection efficiency of DSSCs. It should be noted that there is no serious aggregation of these Ir sensitizers on the semiconductor surface for their non-planar starburst structure.

The photoelectrochemical properties of dyes sensitized TiO_2 electrodes under irradiation of AM 1.5 (100 mW cm^{-2}) are listed in Table 3, while the corresponding photocurrent–voltage curves are shown in Fig. 8. **Ir3** shows the highest conversion efficiency of 2.86%. The open-circuit photovoltage of **Ir2** is dramatically lower than **Ir1** for the adsorption amount of sensitizer **Ir1** is significantly higher than **Ir2** (Table 3), which enables it to form a more compact

Table 3
Performance parameters of dye-sensitized solar cells.

Dyes	J_{sc} (mA/cm^2)	V_{oc} (V)	*ff*	η (%)	Amount[a] (10^{-7} mol cm^{-2})
Ir1	6.31	0.548	0.53	1.84	2.5
Ir1 + DCA	5.48	0.534	0.57	1.67	
Ir2	6.53	0.478	0.55	1.72	0.69
Ir2 + DCA	6.43	0.501	0.55	1.77	
Ir3	9.59	0.552	0.54	2.86	1.44
Ir3 + DCA	9.65	0.524	0.55	2.76	
Ir3[b]	4.31	0.791	0.56	1.91	
N719	17.9	0.622	0.61	6.80	

[a] Amount of the dyes adsorbed on TiO_2 film.
[b] DSSC using Br^-/Br_3^- as redox electrolyte.

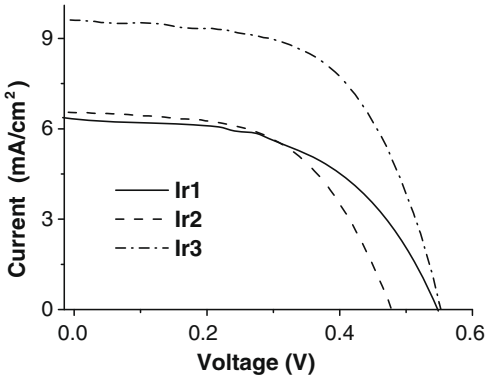

Fig. 8. Photocurrent–voltage curves for DSSCs based on **Ir1**, **Ir2** and **Ir3**.

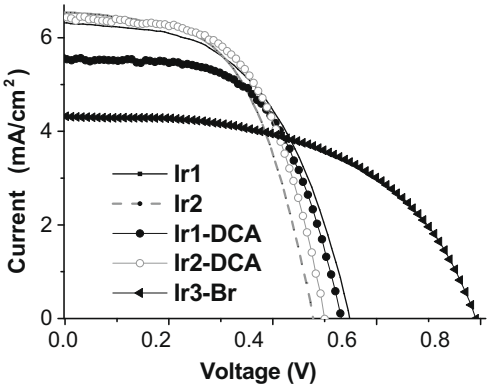

Fig. 9. Photocurrent–voltage (bottom) curves for DSSCs based on **Ir1** and **Ir2** with and without the addition of DCA (1×10^{-3} M) to the dye bath and **Ir3** using Br^-/Br_3^- as redox electrolyte.

sensitizer layer on the semiconductor surface to block the charge recombination [60,61]. In order to further confirm this speculation, the experiment of co-adsorption with deoxycholic acid (DCA), which was usually used to block the charge recombination process, was carried out [62]. The comparative photocurrent–voltage spectra were shown in Fig. 9. The V_{oc} and efficiency of **Ir2** increased distinctly after coadsorbed with DCA, while there is no enhancement for **Ir1** and **Ir3**. With fewer adsorption amount than **Ir1**, the V_{oc} of **Ir3** is similar to that of **Ir1**, which may be caused by the charge recombination suppression capability of the two carboxyl groups of **Ir3** [63].

Br^-/Br_3^- redox electrolyte was employed for **Ir3** and it was found that the V_{oc} was enhanced considerably (Fig. 9). (EBr^-/Br_3^-) is much more positive than (EI^-/I_3^-) and the larger energy gap between the potential of the redox couple and conduction band of TiO_2 can result in larger photovoltage [55]. The more positive potential of **Ir3** in comparison to (EBr^-/Br_3^-) ensures fast electron transfer between the oxidized dye and redox couple. However, for ruthenium dyes such as N719, (EBr^-/Br_3^-) cannot be applied since its relative negative potential cannot ensure sufficient drive force for dye regeneration. The positive potential of Ir complex makes it promising for the enhancement of the photovoltage of DSSCs.

4. Conclusion

A novel type of efficient Ir complex sensitizers with carboxyl pyridine ligand was synthesized, yielding maximum 85% IPCE and 2.86% power conversion efficiency under simulated AM 1.5 sunlight. The results suggest that the energy conversion efficiency can be improved by fine tuning of the spectral overlap between the Ir(III) dye and the solar spectrum. The positive potential of the Ir complexes leads to high photovoltage by employing Br^-/Br_3^- redox electrolyte. The comparison of the luminescence efficiency and electron injection efficiency of the sensitizers indicate that luminescence quantum yield is consistent with the electron injection efficiency of DSSCs, high luminescence quantum yield is favorable to achieve high electron injection efficiency. The control experiment with DCA proved that small size ligand is beneficial for the restraint of the charge recombination in such kind of structure.

Acknowledgements

This work was supported by National Science Foundation of China (50673025), National Basic Research 973 Program (2006CB806200) and Scientific Committee of Shanghai.

References

[1] B. O'Regan, M. Grätzel, Nature 353 (1991) 737.
[2] D.P. Hagberg, J.-H. Yum, H. Lee, F. De Angelis, T. Marinado, K.M. Karlsson, R. Humphry-Baker, L. Sun, A. Hagfeldt, M. Grätzel, M.K. Nazeeruddin, J. Am. Chem. Soc. 130 (2008) 6259.
[3] F. Gao, Y. Wang, D. Shi, J. Zhang, M. Wang, X. Jing, R. Humphry-Baker, P. Wang, S.M. Zakeeruddin, M. Grätzel, J. Am. Chem. Soc. 130 (2008) 10720.
[4] A. Islam, F.A. Chowdhury, Y. Chiba, R. Komiya, N. Fuke, N. Ikeda, K. Nozaki, L. Han, Chem. Mater. 18 (2006) 5178.
[5] Z. Ning, Q. Zhang, W. Wu, H. Pei, B. Liu, H. Tian, J. Org. Chem. 73 (2008) 3791.
[6] M.K. Nazeeruddin, F. De Angelis, S. Fantacci, A. Selloni, G. Viscardi, P. Liska, S. Ito, B. Takeru, M. Grätzel, J. Am. Chem. Soc. 127 (2005) 16835.
[7] W.-Y. Wong, X.-Z. Wang, Z. He, A.B. Djurišić, C.-T. Yip, K.-Y. Cheung, H. Wang, C.S.-K. Mak, W.-K. Chan, Nature Mater. 6 (2007) 521.
[8] A. Islam, H. Sugihara, K. Hara, L.P. Singh, R. Katoh, M. Yanagida, Y. Takahashi, S. Murata, H. Arakawa, G. Fujihashi, Inorg. Chem. 40 (2001) 5371.
[9] E.A.M. Geary, L.J. Yellowlees, L.A. Jack, I.D.H. Oswald, S. Parsons, N. Hirata, J.R. Durrant, N. Robertson, Inorg. Chem. 44 (2005) 242.
[10] W.-Y. Wong, X.-Z. Wang, Z. He, K.-K. Chan, A.B. Djurišić, K.-Y. Cheung, C.-T. Yip, M.-C.N. Alan, Y.X. Yan, C.S.-K. Mak, W.-K. Chan, J. Am. Chem. Soc. 129 (2007) 14372.
[11] W.-Y. Wong, Macromol. Chem. Phys. 209 (2008) 14.
[12] L. Liu, C.-L. Ho, W.-Y. Wong, K.-Y. Cheung, M.-K. Fung, W.-T. Lam, A.B. Djurišić, W.-K. Chan, Adv. Funct. Mater. 18 (2008) 2824.
[13] X.-Z. Wang, W.-Y. Wong, K.-Y. Cheung, M.-K. Fung, A.B. Djurišić, W.-K. Chan, Dalton Trans. (2008) 5484.
[14] S. Ferrere, B.A. Gregg, J. Am. Chem. Soc. 120 (1998) 843.
[15] G. Sauve, M.E. Cass, S.J. Doig, I. Lauermann, K. Pomykal, N.S. Lewis, J. Phys. Chem. B 104 (2000) 3488.
[16] T. Bessho, E.C. Constable, M. Grätzel, A.H. Redondo, C.E. Housecroft, W. Kylberg, Md.K. Nazeeruddin, M. Neuburger, S. Schaffner, Chem. Commun. (2008) 3717.
[17] J.B. Asbury, E. Hao, Y. Wang, T. Lian, J. Phys. Chem. B 104 (2000) 11957.
[18] E.I. Mayo, K. Kilså, T. Tirrell, P.I. Djurovich, A. Tamayo, M.E. Thompson, N.S. Lewis, H.B. Gray, Photochem. Photobiol. Sci. 5 (2006) 871.
[19] A. Juris, V. Balzani, F. Barigelletti, S. Campagna, P. Belser, A. Von Zelewsky, Coord. Chem. Rev. 84 (1988) 85.
[20] Md.K. Nazeeruddin, R. Humphry-Baker, D. Berner, S. Rivier, L. Zuppiroli, M. Grätzel, J. Am. Chem. Soc. 125 (2003) 8790.
[21] G.L. Schulz, S. Holdcroft, Chem. Mater. 20 (2008) 5351.
[22] W.-Y. Wong, C.-L. Ho, Z.-Q. Gao, B.-X. Mi, C.-H. Chen, K.-W. Cheah, Z. Lin, Angew. Chem., Int. Ed. 45 (2006) 7800.
[23] C.-L. Ho, W.-Y. Wong, Q. Wang, D.-G. Ma, L.-X. Wang, Z. Lin, Adv. Funct. Mater. 18 (2008) 928.
[24] W.-Y. Wong, G.-J. Zhou, X.-M. Yu, H.-S. Kwok, B.-Z. Tang, Adv. Funct. Mater. 16 (2006) 838.
[25] P.L. Burn, S.-C. Lo, I.D.W. Samuel, Adv. Mater. 19 (2007) 1675.
[26] R.C. Evans, P. Douglas, C.J. Winscom, Coord. Chem. Rev. 250 (2006) 2093.
[27] G. Zhou, W.-Y. Wong, B. Yao, Z. Xie, L. Wang, Angew. Chem., Int. Ed. 46 (2007) 1149.
[28] B. Carlson, G.D. Phelan, W. Kaminsky, L. Dalton, X. Jiang, S. Liu, A.K.-Y. Jen, J. Am. Chem. Soc. 124 (2002) 14162.
[29] A. Gabrielsson, F. Hartl, H. Zhang, J.R.L. Smith, M. Towrie, A. Vlček Jr., R.N. Perutz, J. Am. Chem. Soc. 128 (2006) 4253.
[30] G. Zhou, C. Ho, W.-Y. Wong, Q. Wang, D. Ma, L. Wang, Z. Lin, T.B. Marder, A. Beeby, Adv. Funct. Mater. 18 (2008) 499.
[31] B. Liang, L. Wang, Y. Xu, H. Shi, Y. Cao, Adv. Funct. Mater. 17 (2007) 3580.
[32] H. Zhen, C. Luo, W. Yang, W. Song, B. Du, J. Jiang, C. Jiang, Y. Zhang, Y. Cao, Macromolecules 39 (2006) 1693.
[33] Q. Zhao, F. Li, S. Liu, M.X. Yu, Z.Q. Liu, T. Yi, C.H. Huang, Inorg. Chem. 47 (2008) 9256.
[34] M.X. Yu, Q. Zhao, L.X. Shi, F.Y. Li, Z.G. Zhou, H. Yang, T. Yi, C.H. Huang, Chem. Commun. (2008) 2115.
[35] P.-T. Chou, Y. Chi, Chem. Eur. J. 13 (2007) 380.
[36] Y. Chi, P.-T. Chou, Chem. Soc. Rev. 36 (2007) 1421.
[37] K.R. Justin Thomas, M. Velusamy, J.T. Lin, C. Chuen, Y. Tao, Chem. Mater. 17 (2005) 1860.
[38] J. Ding, J. Gao, Y. Cheng, Z. Xie, L. Wang, D. Ma, X. Jing, F. Wang, Adv. Funct. Mater. 16 (2006) 575.
[39] D. Qiu, J. Wu, Z. Xie, Y. Cheng, L. Wang, J. Organomet. Chem. 694 (2009) 737.
[40] K.R.J. Thomas, M. Velusamy, J.T. Lin, C. Chien, Y. Tao, Y.S. Wen, Y. Hu, P.T. Chou, Inorg. Chem. 44 (2005) 5677.
[41] S. Lamansky, P. Djurovich, D. Murphy, F. Abdel-Razzaq, H. Lee, C. Adachi, P.E. Burrows, S.R. Forrest, M.E. Thompson, J. Am. Chem. Soc. 123 (2001) 4304.
[42] Y. You, S.Y. Park, J. Am. Chem. Soc. 127 (2005) 12438.
[43] Z. Xu, Y. Li, X. Ma, X. Gao, H. Tian, Tetrahedron 64 (2008) 1860.
[44] C. Hedberg, K. Källström, P. Brandt, L.K. Hansen, P.G. Andersson, J. Am. Chem. Soc. 128 (2006) 2995.
[45] J.D. Slinker, A.A. Gorodetsky, M.S. Lowry, J. Wang, S. Parker, R. Rohl, S. Bernhard, G.G. Malliaras, J. Am. Chem. Soc. 126 (2004) 2763.
[46] T. Sajoto, P.I. Djurovich, A. Tamayo, M. Yousufuddin, R. Bau, M.E. Thompson, Inorg. Chem. 44 (2005) 7992.
[47] S. Liu, Q. Zhao, R. Chen, Y. Deng, Q. Fan, F. Li, L. Wang, C. Huang, W. Huang, Chem. Eur. J. 12 (2006) 4351.

[48] H. Su, H. Chen, F. Fang, C. Liu, C. Wu, K. Wong, Y. Liu, S. Peng, J. Am. Chem. Soc. 130 (2008) 3413.
[49] M.K. Nazeeruddin, A. Kay, I. Rodicio, R. Humphry-Baker, M. Grätzel, J. Am. Chem. Soc. 115 (1993) 6382.
[50] T. Kwon, M.K. Kim, J. Kwon, D. Shin, S. Park, C. Lee, J. Kim, J. Hong, Chem. Mater. 19 (2007) 3673.
[51] A.B. Tamayo, S. Garon, T. Sajoto, P.I. Djurovich, I.M. Tsyba, R. Bau, M.E. Thompson, Inorg. Chem. 44 (2005) 8723.
[52] J.B. Waern, C. Desmarets, L. Chamoreau, H. Amouri, A. Barbieri, C. Sabatini, B. Ventura, F. Barigelletti, Inorg. Chem. 47 (2008) 3340.
[53] C. Yang, S. Li, Y. Chi, Y. Cheng, Y. Yeh, P. Chou, G. Lee, C. Wang, C. Shu, Inorg. Chem. 44 (2005) 7770.
[54] Z.-S. Wang, H. Kawauchi, T. Kashima, H. Arakawa, Coord. Chem. Rev. 248 (2004) 1381.
[55] Z. Wang, K. Sayama, H. Sugihara, J. Phys. Chem. B 109 (2005) 22449.
[56] M.J. Frisch, G.W. Trucks, H.B. Schlegel, P.M.W. Gill, B.G. Johnson, M.A. Robb, J.R. Cheeseman, T. Keith, G.A. Petersson, J.A. Montgomery, K. Raghavachari, M.A. Al-Laham, V.G. Zakrzewski, J.V. Ortiz, J.B. Foresman, J. Cioslowski, B.B. Stefanov, A. Nanayakkara, M. Challacombe, C.Y. Peng, P.Y. Ayala, W. Chen, M.W. Wong, J.L. Andres, E.S. Replogle, R. Gomperts, R.L. Martin, D.J. Fox, J.S. Binkley, D.J. Defrees, J. Baker, J.P. Stewart, M. Head-Gordon, C. Gonzalez, J.A. Pople, GAUSSIAN, Inc., Pittsburgh PA, GAUSSIAN 03, Revision C.01, 2004.
[57] V.A. Montes, C. Perez-Bolivar, N. Agarwal, J. Shinar, P. Anzenbacher Jr., J. Am. Chem. Soc. 128 (2006) 12436.
[58] K. Kilså, E.I. Mayo, D. Kuciauskas, R. Villahermosa, N.S. Lewis, J.R. Winkler, H.B. Gray, J. Phys. Chem. A 107 (2003) 3379.
[59] J. Cornil, D. Beljonne, J. Calbert, J.-L. Brédas, Adv. Mater. 13 (2001) 1053.
[60] M. Yanagida, T. Yamaguchi, M. Kurashige, K. Hara, R. Katoh, H. Sugihara, H. Arakawa, Inorg. Chem. 42 (2003) 7921.
[61] Z.-S. Wang, N. Koumura, Y. Cui, M. Takahashi, H. Sekiguchi, A. Mori, T. Kubo, A. Furube, K. Hara, Chem. Mater. 20 (2008) 3993.
[62] Z. Wang, K. Hara, Y. Dan-oh, C. Kasada, A. Shinpo, S. Suga, H. Arakawa, H. Sugihara, J. Phys. Chem. B 109 (2005) 3907.
[63] K. Hara, H. Sugihara, Y. Tachibana, A. Islam, M. Yanagida, K. Sayama, H. Arakawa, Langmuir 17 (2001) 5992.